

Spectroscopic study of the ϵ phase of solid oxygenFederico A. Gorelli,^{1,3,*} Lorenzo Ulivi,^{2,3,†} Mario Santoro,^{3,‡} and Roberto Bini^{3,4,§}¹*Dipartimento di Fisica dell'Università di Firenze, Largo E. Fermi 2, I-50125 Firenze, Italy*²*Istituto di Elettronica Quantistica, Consiglio Nazionale delle Ricerche, Via Panciatichi 56/30, I-50127 Firenze, Italy*³*LENS, European Laboratory for Non-linear Spectroscopy and INFM, Largo E. Fermi 2, I-50125 Firenze, Italy*⁴*Dipartimento di Chimica dell'Università di Firenze, Via G. Capponi 9, I-50121 Firenze, Italy*

(Received 31 May 2000; revised manuscript received 5 October 2000; published 20 February 2001)

The infrared spectrum of the ϵ phase of solid oxygen has been studied between room temperature and 20 K as a function of pressure up to 63 GPa. Besides the strong absorption in the fundamental O_2 vibron mode and the broad doublet in the overtone region, another peak is detected in the far infrared region. The analysis of the overtone bands allows the determination of the density of states of the O_2 vibron region which consists of two separated energy regions, including one the infrared and the other the Raman bands observed in the 1500–1650 cm^{-1} range. This result, consistent with the analysis of the other Raman and infrared bands at lower frequency, is interpreted on the basis of a crystal composed by a molecular unit formed by four oxygen atoms. This hypothesis explains the strong infrared absorption which is in contrast with the model of a crystal composed by diatomic oxygen molecules. Very thin crystalline slabs ($\leq 0.4 \mu m$) allowed to measure the intensity of the strong infrared absorption at 1500–1550 cm^{-1} . The measurement of the Raman spectrum as a function of the incident power and of the laser excitation frequency shows how the intensity and the frequency of the Raman lines are affected by the experimental conditions. Finally, a simple chain model provides indirect proof of our assignment of the low-frequency infrared mode and allows to rule out an association in polymeric units formed by more than four atoms even at pressures close to the insulator-metal transition.

DOI: 10.1103/PhysRevB.63.104110

PACS number(s): 62.50.+p, 78.30.-j, 61.50.Ks

I. INTRODUCTION

When high pressure is applied to molecular solids impressive phenomena can be observed also in crystals of very simple molecules. The progressive strengthening of the intermolecular interactions on compression can induce, besides a molecular reorientation which generally leads to the achievement of more efficient crystal packing, a reorganization of the molecular chemical bonding. In general, cooperative processes are responsible of the growth of ordered polymeric products, as recently observed for solid CO_2 (Ref. 1) and acetylene.² The formation of different molecular units was, on the contrary, never reported in the past even though an increasing interaction among neighboring molecules has been observed at high pressure in hydrogen,³ nitrogen,⁴ and in a low-pressure phase of oxygen.⁵

The existence of a red colored phase of solid oxygen at room temperature and high pressure was reported by Nicol *et al.* twenty years ago.⁶ The intense coloration of this phase, known as the ϵ phase, is a direct evidence to which extent pressure is capable to modify the electronic properties of a simple molecular crystal. At room temperature oxygen crystallizes in the rhombohedral β phase ($R\bar{3}m$) around 5.7 GPa.^{7,8} A transition to an $Fmmn$ orthorhombic structure (δ phase) is observed near 9.6 GPa.⁹ The β and the δ phases, as well as the low-temperature α phase, possess a peculiar arrangement of the oxygen molecules whose centers of mass sit on layers, coincident with crystal planes, with all the molecular axes perpendicular to these crystal planes. The transition to the ϵ phase takes place around 10 GPa, and also this phase it is characterized by the same layered structure de-

scribed for the lower pressure phases. Two structural investigations on the ϵ phase agree on a monoclinic structure ($A2/m$; $Z=8$), but the exact positions of the molecules and, consequently, the local (site) symmetry are still unknown.^{10,11} In contrast with the several crystalline modifications observed below 10 GPa, the ϵ phase is stable up to 96 GPa where eventually the insulator to metal transition is observed.¹² Besides the intense coloration other important properties characterize the ϵ phase. First, a big volume reduction is observed at the δ - ϵ transition ($\approx 10\%$), essentially due to a contraction in the bc plane which contains the centers of mass of the O_2 molecules.¹³ On the contrary, the transition to the metal takes place with a very small volume decrease ($\leq 1.4\%$). The second important aspect is the appearance of a strong infrared absorption in the fundamental mode region.¹⁴ This observation was associated to the existence of important intermolecular interactions between oxygen pairs which could account for the existence, but not for the intensity, of this absorption. An explanation of the high intensity of the infrared band was attempted by Nicol *et al.* on the basis of optical absorption spectra.¹⁵ They suggested that the out-of-phase stretching mode of the oxygen pairs induces a mixing of the ground state with low-energy ionic states ($O_2^+ - O_2^-$) giving rise to a strong transition dipole moment. Later, Agnew *et al.* proposed a polymeric association for the ϵ phase explaining the vibrational properties on the basis of a simple chain model, based on an O_2 pair unit, with equal intermolecular force constants among the molecules of the pair and the nearest-neighbors molecules of adjacent pairs.¹⁶ The possibility of a chemical bond between two O_2 molecules and the consequent existence of an O_4 molecule has been invoked several times since the beginning

of this century.^{17,18} In these cases the definition of O₄ molecule could be better identified with strongly interacting O₂ – O₂ dimer. The O₂ – O₂ dimers, revealed in the gas-phase by Long *et al.*,¹⁹ are now extensively characterized both from experimental^{20,21} and theoretical^{22–24} point of view. The equilibrium distance of the dimer in the gas is much larger ($\approx 50\%$) than in the ϵ phase at its lower pressure, nevertheless a pronounced energy minimum for the fundamental singlet state, corresponding to a rectangular geometry, is found.²⁵ Recently, we discovered a low-frequency infrared absorption which allowed to conclude that a different tetratomic planar oxygen molecule accounts for the entire, peculiar vibrational properties of the ϵ phase.²⁶

In this paper we want to show how the complete set of vibrational data concerning the ϵ phase of solid oxygen can be interpreted according to a simple model based on a lattice composed by O₄ molecules. Absorption spectra collected in the far infrared, in the O₂ fundamental mode and in the overtone regions provide, together with the Raman data, a complete information on the formation dynamics and on the properties of this molecular unit. A linear chain model based on O₄ units is capable to explain all the data, confirming the assignment of the different bands, and can provide unambiguous proofs of the absence of a further polymeric association prior the insulator to metal transition.

II. EXPERIMENTAL

High-pressure infrared and Raman spectra of solid oxygen were measured using a membrane diamond anvil cell. Oxygen (purity $\geq 99.99\%$) was loaded in the cell by means of cryo-loading equipment. The crystal in the β phase, with a typical thickness of 40–50 μm , was produced by compressing the liquid just above room temperature (≈ 310 K). Care was taken to cross very slowly the melting point in order to obtain high quality crystals. A ruby chip was inserted in the sample to measure the local sample pressure by the R₁ ruby fluorescence band shift according to the equation $P(\text{GPa}) = 248.4[(\lambda/\lambda_0)^{7.665} - 1]$.²⁷

The complete apparatus for infrared experiments, including the optical beam condenser and the cryogenic system, has been extensively described in a previous report.²⁸ Both infrared and Raman set up were the same employed in a previous experiment on nitrogen.²⁹ A Fourier Transform Infrared (FTIR) spectrometer (Bruker IFS-120 HR) was used to measure the infrared spectra. Raman experiments were performed by using as excitation lines the 514.5 and 488 nm emissions of an Ar⁺ and the 647.1 nm emission of a Kr⁺ ion lasers. A double monochromator (U-1000 Jobin Yvon) equipped with a liquid nitrogen cooled CCD camera was used to detect the Raman signal. The instrumental resolution was better than 1 cm^{-1} both in infrared and Raman experiments, while the frequency accuracy was 0.1 cm^{-1} in Raman and much higher (0.005 cm^{-1}) in infrared measurements. The temperature of the sample is measured by a Si diode placed in the copper ring where the diamond is mounted, the resulting uncertainty on the sample temperature is estimated in ± 2 K.

The typical sample diameter is 150 μm and the diffrac-

tion losses are very important below 500 cm^{-1} making the measurement of far-infrared absorption spectra a challenging experiment. For this purpose we built a different focusing system, used in place of our usual cassegrain microscope objectives system, which employs ellipsoidal mirrors as focusing optics. For the far-infrared spectra we used a bolometer as a detector (cooled to 4.2 K) and two different beam splitters depending on the spectral region of interest: a 6 μm thick mylar for the range 100–450 cm^{-1} , and a KBr between 450 and 4000 cm^{-1} .

To measure the intense absorption of the oxygen vibron without saturation we performed midinfrared measurements on sample slabs having an optical thickness ≤ 0.4 μm . This value, necessary to evaluate the absorption coefficient, was calculated by comparing the intensity of the overtone bands with that measured in the pure sample spectra. In this last case the optical thickness could be determined from the period of the interference fringes observed in the spectrum and due to reflections on the diamond windows. These crystalline slabs were prepared by a particular technique, that is filling the gasket hole with NaBr (containing 1% of NaNO₂ for pressure calibration²), pressing it since a transparent pellet was obtained and then, after the surface of this pellet was scratched by means of a thin needle, the cell is filled by the usual cryo-loading technique.

III. RESULTS

We used infrared and Raman spectroscopy to investigate the vibrational properties of solid oxygen in the ϵ phase. For the sake of clarity we will present the data relative to the different techniques in separated subsections.

A. Infrared

Some representative spectra collected in the fundamental vibration region, at different pressures and 50 K, are reported in Fig. 1. The spectrum at 6.3 GPa is measured in the δ phase. Here, beside the quite narrow and weak peak of the fundamental mode around 1550 cm^{-1} , a broad feature is also observed between 1650 and 1750 cm^{-1} which is assigned to the phonon side band.⁵ Above 7 GPa the transition to the ϵ phase can be easily detected by the appearance of a strong band about 15 cm^{-1} below the frequency of the vibron δ peak. The absorption of this band rapidly increases with pressure, and a pronounced shoulder on the low-frequency side of the saturated peak is observed. In a recent infrared study this has been interpreted as due to the presence of four infrared active Davydov components.³⁰ However, this assignment is not very convincing since all the components appeared with the same relative intensity also in spectra recorded on a single crystal with polarized light. For strongly absorbing infrared modes distortions and important asymmetries of the lineshape are frequently observed in the infrared spectra of molecular crystals.³¹ For polar modes angular dispersion (LO-TO splitting) is observed in polycrystalline samples, and in single crystals when the focalization angle is large, as it is common in high-pressure infrared experiments. The second, and more reasonable reason for the

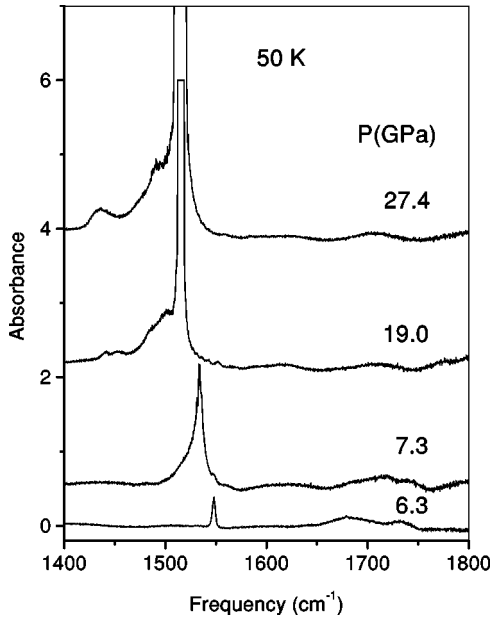


FIG. 1. Low-temperature infrared spectra at different pressures in the fundamental mode region in the δ (6.3 GPa) and in the ϵ phase.

presence of this shoulder in the case of oxygen, is the activation of $k \neq 0$ modes due to the breaking of the translational symmetry caused by lattice defects. This effect could be reasonably expected in experiments at high pressure where the sample undergoes to strong nonisotropic strains unless the single crystal is immersed in an hydrostatic medium like helium. The presence of four infrared bands contrasts with the missed observation of a Davydov splitting for all the other infrared and Raman bands measured in the ϵ phase. In our spectra (see Fig. 1) a weak and narrow peak is observed, below 20 GPa, at lower frequency (around 1450 cm^{-1}). In a previous infrared absorption study performed on isotopic mixtures this band was attributed to the isotope $^{16}\text{O}^{18}\text{O}^{16}$. Around 20 GPa another weak and broad absorption is visible at frequencies just above the isotope peak. The evolution with pressure of the intensity and the position of this absorption band mirrors that of the main saturated peak.

In the δ phase at low temperature, the intensity of the infrared peak was observed to increase very steeply with pressure, revealing an induction mechanism of the dipole moment related to the short-range part of the intermolecular interaction.^{5,32} The high intensity of the vibron peak in the ϵ phase indicates that a different activation mechanism takes place. In fact, we never observed this peak without saturation also reducing the sample thickness down to $20 \mu\text{m}$, unless using the special sample prepared as described above. This result contrasts with the observation reported in Ref. 30 where the main peak was measured without saturation in a polycrystalline sample of thickness $\geq 15 \mu\text{m}$. The measurement of the absorption coefficient is crucial, since the comparison with other systems can help to understand the nature of the transition dipole moment relative to this vibrational mode, but extremely thin crystal slabs are necessary. According to the procedure described in the experimental section we

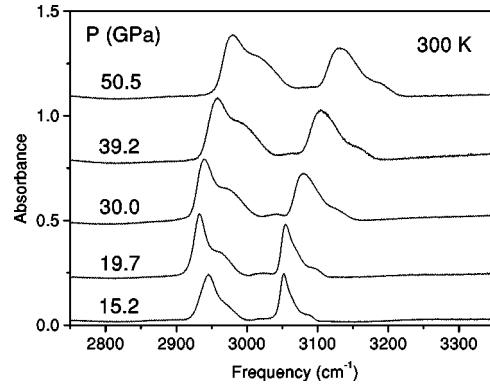


FIG. 2. Room-temperature infrared spectra in the overtone region recorded in the ϵ phase at different pressures.

prepared an oxygen sample having an optical thickness less than $0.4 \mu\text{m}$. With this sample we could measure the absorption of the band at 1500 cm^{-1} up to 24 GPa (Ref. 26) and accordingly calculate the absorbance per unit length $\alpha = \log_{10}(I_0/I)/d$, where the sample thickness d is assumed to be equal to the optical thickness ($\approx 0.4 \mu\text{m}$). It results $\alpha \approx 1.1 \cdot 10^4 \text{ cm}^{-1}$ at 22 GPa, a value which is about one order of magnitude larger than that reported in Ref. 30.

In Fig. 2 the spectra in the overtone region at 300 K and at different pressures are reported. Also in this case, as for the fundamental vibration region, low- and room-temperature spectra are very similar. The independence from temperature of the spectral profile indicates that the overtone absorption essentially reflects the convolution of the density of states (DOS) of the fundamental mode region. The two bands are very similar in shape being constituted, each one, by two peaks with a sharp low-frequency edge and a broader and weaker shoulder on the high-frequency side. From the figure, a different behavior of the frequencies of the two bands is evident. Below 20 GPa the low-frequency band softens while a shift to higher frequencies is common to both bands above 20 GPa. As will be shown in the following, the shifts with pressure are of great help in the assignment of the two bands.

In a previous letter we reported the observation of an intense peak in the far-infrared region.²⁶ According to the side bands observed in the low-temperature spectra of the δ phase, just before the transition to the ϵ phase, we concluded that the one-phonon density of states of the lattice modes extends up to 250 cm^{-1} at the coexistence of the δ and ϵ phases.⁵ The far infrared peak has a frequency greater than 300 cm^{-1} when it appears entering into the ϵ phase, making its assignment to a lattice phonon unreliable. The intensity of this band grows rapidly with pressure but only up to 20 GPa, while above this point its integrated absorption is almost pressure independent.

B. Raman

The room-temperature Raman spectrum of the ϵ phase has been recently reported up to the insulator to metal transition.³³ The spectrum consists of three main bands: a high-frequency peak around 1580 cm^{-1} , assigned to the vi-

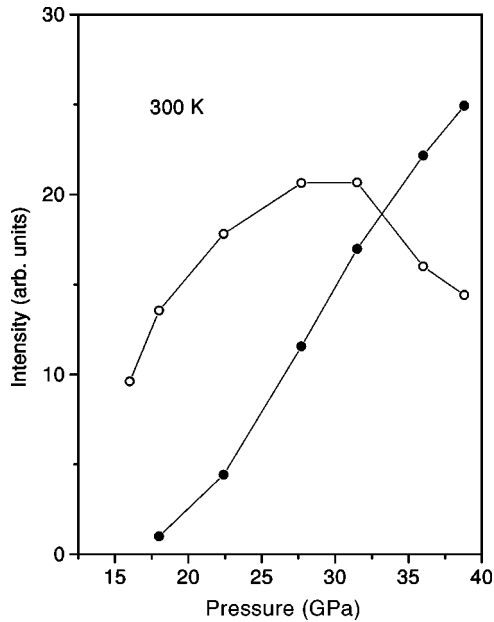


FIG. 3. Integrated intensities of the Raman vibron and L2 modes, empty and full circles, respectively, measured by using as excitation line the 647.1 nm emission of a Kr^+ laser.

bron, and two low-frequency bands (below 500 cm^{-1}) interpreted as two librons (L1, L2). The pressure evolution of the intensities of all the modes shows a maximum, particularly pronounced for the L2 band, between 25 and 35 GPa. This maximum was attributed to resonance Raman effects, since the 514.5 nm line of an Ar^+ ion laser was used as source. In fact, being ϵ -oxygen crystals deeply red, the green light is strongly absorbed determining also a heating of the sample. In order to avoid this heating we repeated the experiment by using the red line of a Kr^+ ion laser (647.1 nm), which is weakly absorbed by the sample, with a maximum power of 0.5 W. We measured polycrystalline ϵ samples at room temperature up to 39 GPa by using different laser powers and excitation wavelengths, in order to identify the effects of laser heating. The first result concerns the evolution of the intensities with pressure of all the bands which appears to be independent from the excitation wavelength. In Fig. 3, the Raman intensities of the L2 and the vibron peaks, obtained with Kr^+ laser source, are reported up to 39 GPa. The evolution with pressure of the two sets of data is very similar to that reported in Fig. 2 of Ref. 33 obtained with the 514.5 nm excitation line. This suggests that the maximum of the Raman intensity of the vibron, observed around 30 GPa, cannot be fully ascribed to resonance effects. We also revealed frequency shifts of some tens of wavenumbers for all the bands depending on the power and on the wavelength of the excitation line, remarking how important is the heating effect due to the laser absorption. The frequencies of the three bands reported in Ref. 33 were always larger (up to 20 cm^{-1} at 39 GPa) than our data. This is a very important aspect to decide the assignment of the low-frequency Raman bands in relation to the infrared results.

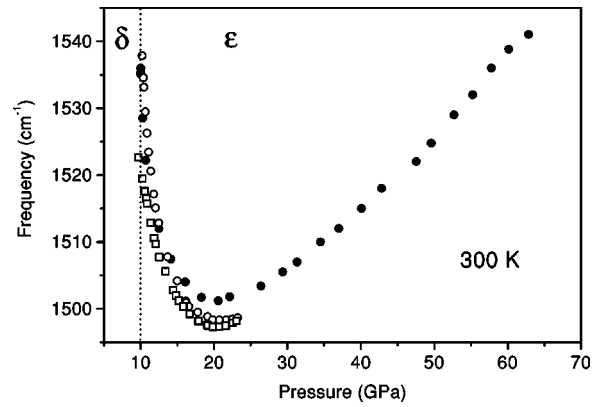


FIG. 4. Room temperature frequency evolution with pressure of the infrared MIR peak. Full dots are obtained from an estimation of the position of the saturated peak in the pure oxygen spectra. Empty symbols are relative to the thin oxygen sample spectra increasing (dots) or releasing (squares) pressure.

C. Frequency and intensity analysis

The analysis of infrared and Raman spectra was performed by fitting with pseudo-Voigt profiles the bands of interest. Frequency, linewidth and integrated absorption, or relative intensity for the Raman bands, could be obtained. For the thick samples the frequency of the infrared vibron peak at 1500 cm^{-1} (MIR band) could be only estimated from the saturated peak. A precise determination was possible only in the experiments on the thin sample. The frequencies values of the MIR peak obtained, at room temperature, with the two procedures are presented in Fig. 4. The data obtained in the experiment on the thin sample (open symbols) are in good agreement with the values estimated from the saturated peak (solid dots). From the figure it appears that the frequency of this peak shows a surprising behavior when pressure increases. After the δ - ϵ phase transition the frequency rapidly decreases, of about 50 cm^{-1} , approaching a minimum around 20 GPa, then it grows slowly up to the highest pressure of this experiment, 63 GPa. This behavior was not observed by Agnew *et al.*,¹⁶ whose measurement was extended only up to 20 GPa. They concluded, from the observed monotonic softening, that the O-O bond continuously weakens rising pressure. The present evolution of the MIR peak with pressure, which is almost identical also at low temperature, was described in our previous report³⁴ and recently confirmed by other studies,^{26,30} indicates that the process is more complex.

The position of the peak observed in the far infrared region (FIR band) has a completely different pressure evolution. In the region between 10 and 20 GPa, characterized by the big softening of the MIR mode, the frequency of the FIR mode increases steeply ($10\text{ cm}^{-1}/\text{GPa}$). The frequency behavior with pressure of all the infrared and Raman modes measured in the present work is shown in Fig. 5. For comparison also the Raman data from a recent work by Akahama *et al.*³³ are shown. The frequency of the Raman vibron is almost constant up to 15 GPa, then it rises linearly with pressure up to the transition to the metallic phase (96 GPa).¹² Furthermore, it is also characterized by a steeper dependence

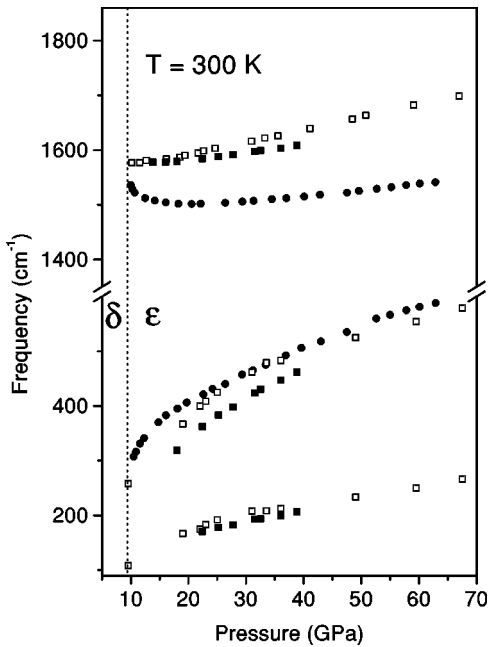


FIG. 5. Frequencies of the Raman and infrared modes of ϵ oxygen. Dots refer to the ν_{MIR} and ν_{FIR} modes, squares to the vibron, L2 and L1 Raman modes. Full symbols refer to our measurements while open symbols refer to data from Ref. 33.

on pressure ($\approx 2.5 \text{ cm}^{-1}/\text{GPa}$) than that of the MIR peak ($\approx 1.1 \text{ cm}^{-1}/\text{GPa}$) above 35 GPa. The evolution with pressure of the low-frequency L1 and L2 Raman modes recalls quite closely that of the FIR mode. It is important to remark the difference, concerning the frequency position of the L2 peak, between our data (full squares) and those from Ref. 33 (empty squares). Our data discredit any speculation on the possible coincidence of the L2 and the FIR peaks and, consequently, the possibility that the two peaks are due to the same crystal mode, showing both infrared and Raman activity, can be ruled out. Therefore, the ϵ phase seems to be characterized by two pressure regions. From the δ - ϵ phase transition (10 GPa) up to 20 GPa all the modes show quite different evolution. Above 20 GPa, although with different slopes, all the frequencies increase with pressure. The different behavior of the Raman vibron and of the MIR peak can be hardly explained considering them as crystal components (Davydov splitting) of the same stretching mode of the isolated molecule.

Quantitative information can be obtained by the integrated absorption of the two infrared modes. In fact these data, after a renormalization with respect to the optical thickness and density, provide a powerful tool to understand the nature of the strong infrared activity in the ϵ phase by comparison with infrared active vibrational modes of other molecular crystals. The experiment on the thin slab allows to obtain the integrated absorption also for the strong MIR mode. The quantity $\chi = I/\rho nd$, where I is the integrated mode intensity, ρ is the density¹³ and nd is the optical thickness, calculated according to the procedure described in the experimental section, was computed for both modes. This normalized intensity obtained for the MIR mode of ϵ oxygen

at 20 GPa is $\chi = 13 \cdot 10^4 \text{ cm/g}$.³⁵ This value, extraordinarily large for a diatomic homonuclear molecule which can borrow infrared activity only from crystal field effects, is typical of infrared allowed transitions in isolated molecules like CO_2 ($\chi = 31.40 \cdot 10^4 \text{ cm/g}$) and N_2O ($\chi = 15.85 \cdot 10^4 \text{ cm/g}$).³⁶

D. Analysis of the overtone bands

The presence of two absorption bands in the overtone region was mentioned by Swanson *et al.*¹⁴ Before assigning the spectral features of this region some elements necessary to the discussion should be defined. Since the separation between the Raman and the infrared MIR peaks in the fundamental O_2 vibration mode increases continuously with pressure (100 cm^{-1} at 23 GPa; 150 cm^{-1} at 63 GPa), we identify the DOS close to the optical infrared and Raman modes as $IR(k)$ and $R(k)$, respectively. Agnew *et al.* assigned the low-frequency overtone band to the combination of Raman and infrared zone boundary ($k = \pi/a$) vibrational modes with opposite wave vectors: $R(k) + IR(-k)$. The higher-frequency band was on the contrary assigned to the combination of the infrared and Raman $k=0$ modes.¹⁶ The frequencies of the overtone bands calculated according to this assignment are higher than those experimentally observed. The authors had to scale down of $20\text{--}25 \text{ cm}^{-1}$ the calculated values in order to reproduce the measured overtone frequencies justifying this procedure by considering the anharmonicity of the isolated molecule. The strong limit of this assignment is that the combination of two crystal modes, with the only exception of bound states, are not affected by the single molecule anharmonicity.³¹ As already pointed out our spectra of the overtone region (see Fig. 2) show two separated broad absorptions having a similar shape. The width of the low-frequency (LF) band is systematically 1.5 times larger than the high-frequency (HF) one, and the frequency behavior with pressure of the two bands is very different. Between the δ - ϵ phase transition and 20 GPa the LF band moves to lower frequencies while, at higher pressures it hardens, mirroring the frequency evolution of the fundamental MIR mode. On the contrary the frequency of the HF peak is practically unchanged below 20 GPa and grows faster than the LF band above this pressure value. On this basis we suggested a different interpretation of the two bands assigning the LF band to the combination of two delocalized infrared vibron excitations having opposite wavevectors [$IR(k) + IR(-k)$], while the HF band is due to the combination of infrared and Raman active vibron modes with opposite wavevectors [$R(k) + IR(-k)$].³⁴

Following this assignment, the profiles of the LF band is the convolution of the infrared density of states with itself, while the HF band is the convolution of the infrared and the Raman density of states. On this basis we can extract these latter from the spectra. In this procedure we used the minimum amount of gaussian bands to simulate the fundamental infrared and Raman DOS and reproduce analytically the experimental overtone spectra. The sum of two gaussians, for both DOS, sufficed to provide the experimental spectral shape of the overtone bands at every pressure. According to

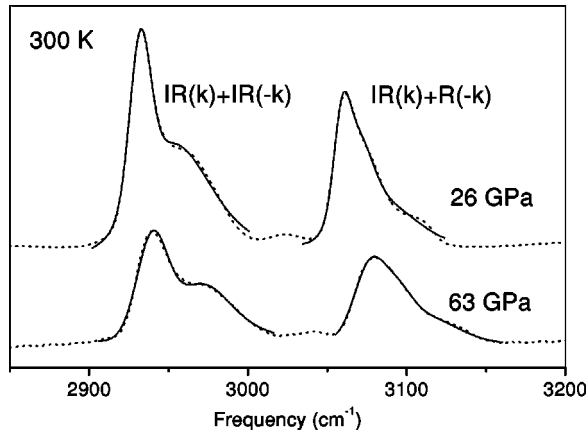


FIG. 6. Fit of the overtone bands at 26 and 63 GPa and room temperature. Dashed and full lines represent experimental and calculated spectra, respectively.

this model the $IR(k)+IR(-k)$ and the $R(k)+IR(-k)$ combination bands are composed by three and four Gaussians, respectively. We performed a nonlinear fit procedure, to reproduce the overtone spectral profiles, by using as adjustable parameters the position, amplitude and width of the four gaussians, which constitute the IR and the Raman vibron DOS. The excellent agreement obtained at all the investigated pressures is a direct confirmation of our assignment. In Fig. 6 the results of the fit at two different pressures are shown.

E. Determination of the vibron density of states

From the analysis of the overtone bands described in the previous paragraph we extract the vibron density of states of the infrared and Raman modes. These DOS are reported in Fig. 7(a), at three different pressures, together with the peak position of the experimental bands (vertical lines). The infrared and Raman density of states are quite similar in shape being constituted by a low-frequency intense peak and a high-frequency broader and weaker peak. The dispersion of the DOS relative to the infrared mode is always 1.5–2 times greater than that corresponding to the Raman band. The optical vibron modes lies always on the high-frequency side of the two DOS which are separated by a well pronounced gap. The presence of this gap is a very surprising result if one wants to interpret the full density of states as arising from one single molecular mode. This would be the only case, to our knowledge, where such effect is observed in molecular crystals. As an example we report in Fig. 7(b) the infrared and Raman calculated DOS together with the experimental spectra at 25 GPa. It can be observed that the calculated frequency dispersion of the infrared DOS is in good agreement with the experimental infrared absorption.

By performing the deconvolution of all the spectra we have determined the profiles of the DOS at every pressure and, consequently, we were able to follow the evolution of the gap with pressure, shown in Fig. 8. To extract a numerical value, the limit of each DOS was conventionally set where the intensity value was less than the 5% of the peak

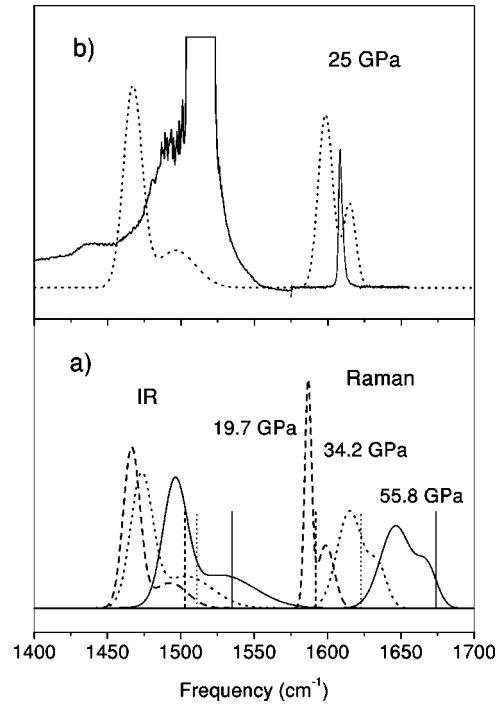


FIG. 7. (a): Density of states of the Raman and infrared modes resulting from the deconvolution of the overtone combination bands at 19.7 (dashed), 34.2 (dotted), and 55.8 (full) GPa. Vertical lines indicate the position of the $k=0$ infrared and Raman modes. (b): Experimental infrared and Raman spectra at 25 GPa compared with the calculated DOS at the same pressure.

maximum. The gap reaches a maximum around 20 GPa and decreases almost linearly at higher pressures.

IV. DISCUSSION

All the results, presented in the previous sections, concerning the vibrational properties of the ϵ phase are hardly interpreted on the basis of a crystal of simple O_2 molecules. It is well known that one of the characteristic features of the crystal structures of oxygen, with the only exception of the γ phase, is the parallel alignment of the closest neighbor molecules.¹⁵ At the $\delta-\epsilon$ phase transition a strong volume

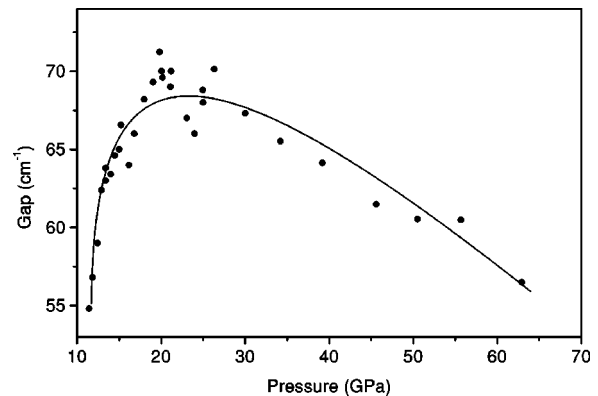


FIG. 8. Evolution with pressure of the gap between the IR and Raman density of states. The solid line is an eye guide and not a fit.

reduction is observed, essentially driven by a contraction in the bc plane where the centers of mass of the parallel oxygen molecules are contained.¹³ The main consequence is a consistent reduction of the nn distance, which, assuming a δ -type layer structure, is about 2.4 Å at 13.7 GPa. A suggestive hypothesis to explain the appearance of the infrared peaks and the complex shape of the infrared and Raman DOS in the fundamental mode region of the O₂ molecule is provided by the existence of a more complex molecular unit. According to the previous considerations, the simplest molecular structure consists of an oxygen unit composed by four atoms and a rectangular geometry. The formation of this unit follows a progressive stronger interaction between nearest-neighbor O₂ molecules. In fact, we already reported how important are charge transfer mechanisms at lower pressures, in the δ phase,^{5,32} where the distances among the closest molecules are larger than 2.55 Å.^{9,37} Moreover the appearance of a diffraction line at 4.48 Å in the ϵ phase proves that the primitive cell has doubled,³⁷ and considering the negligible interplanar distance decrease at the transition, it is reasonable to conclude that this doubling has occurred along one of the two axes of the molecular oxygen plane.¹⁶ Between 13.7 and 35 GPa, the distances between the nearest-neighbors molecules in the bc plane farther decrease of $\approx 10\%$ (being of the order 2.2 Å at 35 GPa), while the distances between closest oxygen atoms of molecules sitting in different planes are always larger.³⁷ These pure geometrical considerations suggested that this molecule derives from the bonding between nearest-neighbor molecules in the bc plane.²⁶

A. O₄ model

According to the previous structural considerations the geometry of the O₄ unit can be confidently considered rectangular, i.e., having a D_{2h} symmetry. The same geometry was recently found to be the most stable also for the (O₂–O₂) dimers in the gas phase, with a pronounced well (200 K) for the fundamental singlet state where the molecules are separated by 3.56 Å.²¹ Also high resolution electronic data of O₂–O₂ dimers in a solid neon matrix at 4 K suggest this geometry with a distance between the molecules of 3.41 Å.²⁰ The existence of O₄ molecules in the gas phase has been also proposed to explain the red light emission, observed in the chemical oxygen iodine laser.³⁸ Several reports on the cooperative absorptions and emissions of the O₂ molecule account for strong intermolecular interactions which can be read on the basis of tightly bound O₂–O₂ dimers. For instance, Dianov-Klokov reported on a number of experiments measuring the cooperative absorption bands of oxygen under a variety of conditions.³⁹ The radiative lifetime of the O₄ complex has been estimated by Bernard *et al.*⁴⁰ Finally, Bussery *et al.* computed an *ab initio* intermolecular potential for (O₂)₂ dimer.²⁴ They found that the lowest energy corresponds to a parallel planar D_{2h} geometry for the singlet state ($\Delta E_{min} = -221$ K at $R_e = 3.2$ Å) and conclude that the (O₂)₂ dimer is indeed a weakly bound molecule with hindered rotation around its van der Waals bond.

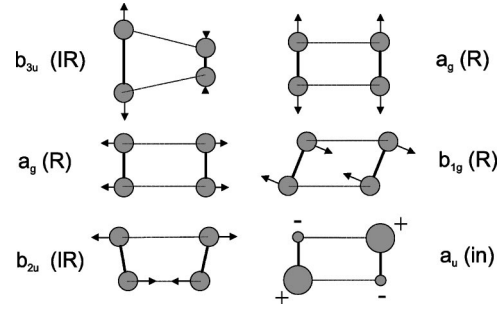


FIG. 9. Normal modes, with relative symmetry and activity, of an O₄ molecule having D_{2h} symmetry.

As already pointed out in the ϵ -oxygen crystal the separation between neighboring molecules in the bc plane is surely less than 2.4 Å (for $P \geq 13.7$ GPa) therefore at least 30% lower than the dimer equilibrium distances, making reasonable the picture of an O₂–O₂ bond. Six normal vibrational modes are expected for this O₄ unit. For a rectangular D_{2h} geometry these modes are shown in Fig. 9: a symmetric (a_g) and an antisymmetric (b_{3u}) stretching mode involving the internal O–O bond, two analogous symmetric (a_g) and antisymmetric (b_{2u}) stretching modes involving the O₂–O₂ bonds, and one in-plane (b_{1g}) and one out-of-plane (a_u) bending modes.

A calculation on a hypothetical O₄ molecule using density functional theory, (B3LYP functionals) with the 6-31G(D) basis set (GAUSSIAN rev E.2),⁴¹ gave as result a rectangular planar structure with a distance between the O₂ units of 1.95 Å.⁴² This distance is shorter than the separation between closest O₂ units which changes, assuming a layered structure as in the δ phase, from 2.4 (14 GPa) to about 2.0 Å just before the insulator to metal transition at 96 GPa.¹³ The results of this calculation, reported in Table I, should be considered just as a qualitative guide for the interpretation of our spectra. The symmetric stretching (a_g) and the antisymmetric (b_{3u}) mode, calculated at 1634 and 1465 cm⁻¹, can be assigned to the Raman and infrared modes observed in the crystal at 1590 and 1500 cm⁻¹ (20 GPa), respectively. It follows that the infrared and the Raman peaks are not the Davydov components of the O₂ stretching mode, but are originated by two different modes in the isolated O₄ molecule. The experimental separation between the two bands is comparable to that obtained in the simulation (≈ 170 cm⁻¹) only at quite high pressure

TABLE I. Calculated frequencies and relative symmetries, of the vibrational mode of the O₄ molecule (Ref. 42), a.s. and s.s. are, respectively, the antisymmetric and the symmetric stretching modes, while o.o.p. bend. and i.p. bend. indicate, respectively, the out-of-plane and in-plane bending modes.

Mode	Symmetry	ν (cm ⁻¹)	Activity	IR int.(arb.units)
a.s. (O–O)	b_{3u}	1465	IR	431
s.s. (O–O)	a_g	1634	Raman	-
o.o.p. bend.	a_u	541	inactive	-
i.p. bend.	b_{1g}	804	Raman	-
a.s. (O ₂ –O ₂)	b_{2u}	205	IR	19
s.s. (O ₂ –O ₂)	a_g	524	Raman	-

(150 cm^{-1} at 60 GPa), where the distance between closest neighbor O_2 units is estimated to be approximately 2.15 \AA . Following this scheme, the two low frequency Raman bands L_1 and L_2 can be assigned, respectively, to the in-plane bending (b_{1g}) and to the symmetric stretching of the $\text{O}_2 - \text{O}_2$ bonds (a_g). The corresponding antisymmetric mode b_{2u} is expected in a very low-frequency region, therefore we assign the peak observed in the far infrared region to this mode. From this picture it derives that all the bands observed below 1600 cm^{-1} can be assigned to fundamental modes of the isolated O_4 molecule. The assignment of the L_2 and FIR bands, respectively, to the symmetric and antisymmetric stretching modes along the $\text{O}_2 - \text{O}_2$ bonds is also supported by their intensity evolution with pressure. In fact, the intensity of these modes increases enormously up to 20–30 GPa indicating a progressive strengthening of these bonds.^{26,33}

Another information obtained by the calculations concerns the infrared activity of the antisymmetric stretching modes. Both modes are infrared allowed, by symmetry, in the isolated molecule, so that an infrared activity is expected in the crystal, as it is indeed observed. However, in order to account for the large transition dipole moment of the mid-infrared stretching mode, other mechanisms should be considered. The simplest hypothesis takes into account charge transfer processes, already discovered in the lower-pressure δ phase, which are responsible of the $\text{O}_2 - \text{O}_2$ bond formation.^{5,32} This process can produce a charge density oscillation which could justify the strong experimental absorption.

Also the peculiar shape of the overtone region can be interpreted on the basis of the O_4 molecule model. Once the two Raman and infrared bands in the $1500\text{--}1600 \text{ cm}^{-1}$ region are assigned to different stretching modes of the O_4 molecule, respectively a_g and b_{3u} , it is easy to understand the two distinct density of states in the crystal as deriving from the two fundamental modes. Therefore, from this model we immediately explain the existence of a gap between the *IR* and Raman vibron density of states but we can not provide any insight on its peculiar behavior with pressure. In the section dedicated to the frequency analysis we emphasized how peculiar is the evolution with pressure of ν_{MIR} and how different it is from that of the low-frequency FIR mode. The remarkable softening of the high-frequency mode clearly indicates a weakening of the force constants involved in the corresponding vibrational motion. From Fig. 9 we can observe that the force constant involved in the b_{3u} vibration is mainly the one related to the original O_2 bonds, which implies that the O_2 bond progressively weakens between 10 and 20 GPa. In the same pressure range, on the contrary, we observe that the FIR mode (b_{2u}) has a strong hard behavior suggesting that the force constant relative to the $\text{O}_2\text{-O}_2$ bonds is increasing. The similar evolution of the two modes above 20 GPa indicates that the process leading to the formation of the O_4 molecule is complete. These conclusions agree also with the intensity evolution of the low-frequency infrared and Raman modes which can be interpreted as a sort of “dynamic” information on the bond formation. As a matter of fact, on this basis we can also

understand the frequency gap behavior which increases up to 20 GPa mirroring the dynamics of the O_4 molecule formation. At higher pressure the progressive decrease in the gap suggests that the interactions among the O_4 units of the crystal are growing. An extensive discussion of this point will be given in the next paragraph.

The charge density oscillation which is at the basis of the strong *IR* absorption can also explain the different behavior of the frequency of the infrared and Raman high-frequency modes between 10 and 20 GPa. Contrary to the remarkable softening of the infrared mode the frequency of the Raman peak increases very weakly in the same pressure range. For nonconducting charge transfer (CT) molecular crystals an electron-molecular vibration coupling model (e-mv) has been successfully applied to describe the infrared absorption of the out of phase CT pair mode and the frequency of both symmetric and antisymmetric vibrational modes.⁴³ In the case of a linear stack of dimers, this model predicts that the frequency of the out of phase mode alone is affected by the e-mv interaction and a strong infrared activity for the same mode is expected. On the contrary in the case of a regular stack, in which each molecule has two neighbors at the same distance no infrared intensity is predicted. Also this result nicely agrees with a description of the ϵ phase in terms of O_4 molecular units.

At this stage of the discussion it is important to remark that the two infrared bands around 3000 cm^{-1} are, respectively, the overtone (*IR+IR*) of the antisymmetric stretching mode (b_{3u}) and the combination of the two stretching modes involving the original O_2 internal bonds ($a_g; b_{3u}$). This assignment suggests an immediate question on the origin of the intensity of the *IR+IR* band. In fact the intensity of a two quanta excitation generally agrees with the activity expected according to symmetry arguments.³¹ This means that the first overtone bands should not be observed in the infrared spectrum of crystals of centrosymmetric molecules. A possible explanation for the presence of this band in this spectrum is that the O_4 molecule is slightly distorted with respect to a perfect rectangular geometry, and consequently loses the inversion symmetry. A C_{2v} molecular symmetry suffices to account for our infrared data, and only a very small tilt of the molecular axis of the O_2 units forming the O_4 molecule is required.

Finally, on the basis of this model we can draw some conclusions on the magnetic properties of the ϵ phase. In the α phase the exchange intermolecular interaction for a couple of neighboring molecules determines an antiferromagnetic order.⁴⁴ Also for the δ phase, which was expected to be antiferromagnetic as the α phase,⁴⁵ this magnetic order was recently demonstrated.³² *Ab initio* calculations expect a pressure induced magnetic collapse at high pressure as the result of the increase of electron hopping and charge transfer interaction.⁴⁶ At the $\delta\text{--}\epsilon$ phase transition the distance between two O_2 molecules decreases, originating a spin pairing process with the change of the electronic structures due to the formation of the O_4 molecule. This picture would also imply a magnetic collapse at the transition, and the ground state of the O_4 molecule would possibly be a singlet.

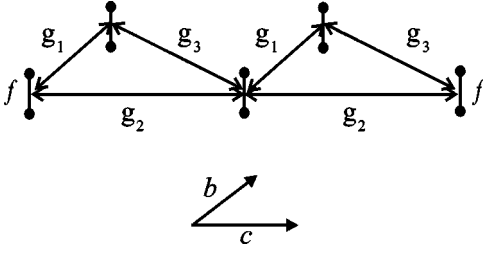


FIG. 10. Linear chain of O_4 molecules in the bc plane. The interactions are described by the force constants f , g_1 , g_2 , and g_3 .

B. Structural model: Linear chain of O_4 molecules

In the previous paragraph we have demonstrated that all the vibrational properties of the red phase of oxygen can be explained on the basis of the formation of an O_4 molecule. A primitive cell constituted by a single O_4 molecule explains also the absence of Davydov splitting of all the observed modes. All the arguments used to interpret the vibrational spectra of this phase are still valid if we assume a polymeric association in the bc plane, having as a monomeric unit the O_4 molecule. This arrangement is extremely intriguing for two reasons. First, an efficient electronic delocalization could account for the intense red color of the crystal as it is observed in polymerization processes of simple molecules like acetylene.⁴⁷ Second, a polymeric arrangement in the bc plane could be the first step in the metallization process and could explain the small structural changes at the insulator to metal transition ($\Delta V/V \approx 1\%$).¹³

According to the structural information, the simplest approach to discuss the formation of a polymer is to consider a linear chain of O_4 molecules. A similar method was used by Agnew *et al.*¹⁶ who considered a linear chain having as basis unit two parallel O_2 molecules at equal distance. This approach was used to reproduce the overtone region according to an assignment different from the one favored in this paper, as discussed in a previous section. They obtained two very different dispersion curves for the infrared and Raman modes, with the dispersion of the Raman mode about four times larger than the infrared one, and a crossing of the two curves at the zone boundary. The resulting density of states, which extends continuously between 1490 and 1580 cm^{-1} ,¹⁶ is in striking contrast with the one derived from the overtone bands. Our chain model is based on the assumption that the two molecules which associate in the ϵ phase are the nearest neighbors in the δ phase. This determines a structure relative to the bc plane of the ϵ phase as that qualitatively described in Fig. 10. The dispersion curves, along the chain axis, of the infrared and Raman active modes, can be calculated by considering each O_2 molecule as an oscillator, with a natural frequency $\nu = (1/2\pi)\sqrt{f/\mu}$, where f is the internal force constant and μ the reduced mass of the oxygen molecule. Each oscillator is allowed to interact with the neighbors, and their coupling is represented by the force constants g_1 , g_2 , and g_3 . The O_4 unit is formed by two O_2 molecules coupled by the g_1 force constant, while g_2 and g_3 couple the vibrations of molecules sitting in nearest-neighbor primitive cells.

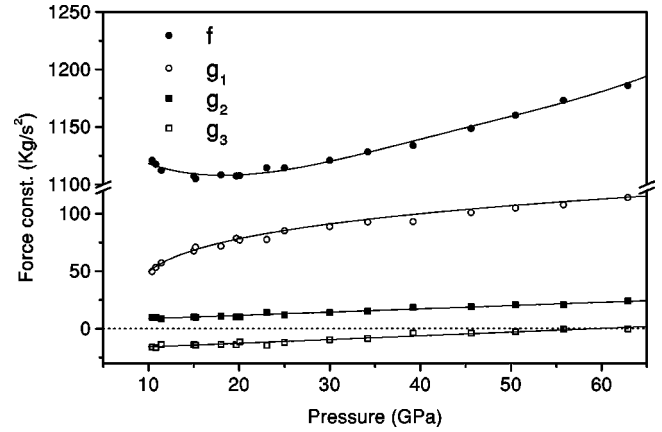


FIG. 11. Pressure evolution of the force constants values obtained by the linear-chain model.

If L is the distance between nearest-neighbor (nn) unit cells, and we consider only the interaction among the oscillators present in these cells, the dynamical matrix results:⁴⁸

$$D(k) = \frac{1}{\mu} (F_0 + F_1 e^{ikL} + F_{-1} e^{-ikL}), \quad (1)$$

where F_0 , F_1 , F_{-1} are the force constants matrix which characterize the interaction forces between oscillators of the same and of nn unit cells, respectively. Therefore:

$$D(k) = \frac{1}{\mu} \begin{pmatrix} f & g_1 \\ g_1 & f \end{pmatrix} + \frac{e^{ikL}}{\mu} \begin{pmatrix} g_2 & 0 \\ g_3 & g_2 \end{pmatrix} + \frac{e^{-ikL}}{\mu} \begin{pmatrix} g_2 & g_3 \\ 0 & g_2 \end{pmatrix} \\ = \frac{1}{\mu} \begin{pmatrix} f + 2g_2 \cos kL & g_1 + g_3 e^{-ikL} \\ g_1 + g_3 e^{ikL} & f + 2g_2 \cos kL \end{pmatrix}. \quad (2)$$

The dispersion curves of the Raman and infrared modes are obtained from the diagonalization of the dynamical matrix:

$$\nu_R^2(k) = \frac{1}{4\pi^2\mu} (f + 2g_2 \cos kL + \sqrt{g_1^2 + g_3^2 + 2g_1g_3 \cos kL}) \quad (3)$$

$$\nu_{IR}^2(k) = \frac{1}{4\pi^2\mu} (f + 2g_2 \cos kL - \sqrt{g_1^2 + g_3^2 + 2g_1g_3 \cos kL}). \quad (4)$$

The two frequencies ν_R and ν_{IR} correspond, respectively, to the in- and out-of-phase vibration of the two O_2 molecules in the unit cell. If $g_3 = 0$ and $f \gg g_1 > g_2 > 0$ from Eqs. (3) and (4) it results that g_1 is responsible for the mode splitting for every k , while g_2 determines the dispersion of the two modes. Therefore, if $g_3 = 0$, the gap exists only if $g_1 > 2g_2$. If $g_3 \neq 0$ the dispersions of the two modes are no longer equal and in order to obtain an *IR* dispersion greater than the Raman one, as obtained from the experiment (see Fig. 7), a negative value of g_3 is necessary. The values of the four force constants f , g_1 , g_2 , and g_3 are related to the values of the Raman and *IR* frequencies at $k=0$ and at the zone boundary ($k = \pi/L$) according to the following relations:

$$f = \pi^2 \mu \left[\nu_R^2(0) + \nu_{IR}^2(0) + \nu_R^2\left(\frac{\pi}{L}\right) + \nu_{IR}^2\left(\frac{\pi}{L}\right) \right] \quad (5)$$

$$g_1 = \pi^2 \mu \left[\nu_R^2(0) - \nu_{IR}^2(0) + \nu_R^2\left(\frac{\pi}{L}\right) - \nu_{IR}^2\left(\frac{\pi}{L}\right) \right] \quad (6)$$

$$g_2 = \frac{\pi^2 \mu}{2} \left[\nu_R^2(0) + \nu_{IR}^2(0) - \nu_R^2\left(\frac{\pi}{L}\right) - \nu_{IR}^2\left(\frac{\pi}{L}\right) \right] \quad (7)$$

$$g_3 = \pi^2 \mu \left[\nu_R^2(0) - \nu_{IR}^2(0) - \nu_R^2\left(\frac{\pi}{L}\right) + \nu_{IR}^2\left(\frac{\pi}{L}\right) \right]. \quad (8)$$

We can observe that g_1 is related to the average splitting between the Raman and *IR* modes, while g_2 and g_3 are responsible, respectively, for the average and the different dispersions of the two modes. Using the experimental $k=0$ Raman and *IR* frequencies and the zone boundary values of the vibron modes DOS, as extracted from the deconvolution procedure of the overtone bands, we can calculate, by using Eqs. (5)–(8), the force constants at all the experimental pressures. The relative weight of the coupling force constants at 20.1 GPa is $g_1/f \approx 7\%$ and $g_2/f \approx g_3/f \approx 1\%$, while in the δ phase at 7 GPa we obtain $G/f \approx 0.4\%$, indicating an increase of the coupling force constant, from δ to ϵ , of a factor ≈ 20 .⁵ The coupling force constant between the two O_2 units which constitute the O_4 molecule at 20 GPa is seven times greater than the one between O_2 units of different O_4 molecules. These values confirm that the ϵ phase is composed by O_4 molecules characterized by two quite different intramolecular forces which are, however, much stronger than those (intermolecular) among different O_4 units.

These conclusions are better illustrated by the force constants evolution with pressure reported in Fig. 11. The internal (O_2 bond) force constant f decreases between 10 and 20 GPa, while in the same pressure range g_1 increases of more than 50%. This behavior exactly mirrors the frequency evolution of the MIR and FIR modes, respectively, and it supports our interpretation of a weakening of the internal O_2 bond and of a corresponding hardening of the bond between adjacent O_2 units leading to the formation of the O_4 molecule. The identical evolution of g_1 respect to the frequency of the far infrared band (Fig. 5) also confirms the assignment of this peak to the intermolecular asymmetric stretching mode. As to g_2 , responsible for the average dispersion of the vibron modes, and g_3 , they increase almost linearly with pressure but with a small slope, indicating that the two vibron modes have a comparable dispersion at high pressure. Even though our results are limited to 63 GPa, we can observe that at this pressure the value of g_1 is much larger than those of g_2 and g_3 . An association among O_4 molecules requires that both the intermolecular force constants g_2 and g_3 approach the g_1 value. Therefore, these results confirm

the validity of the molecular O_4 model for the whole ϵ phase and exclude a further, polymer-type, association.

V. CONCLUSIONS

The infrared spectrum of solid ϵ oxygen has been studied up to 63 GPa between 100 and 3500 cm^{-1} in the temperature range 20–300 K. Three different absorption regions are identified. A low-frequency band, below 500 cm^{-1} , which moves rapidly with pressure to higher energies especially between 10 and 20 GPa. In the same pressure range the frequency of the strong absorption in the O_2 fundamental mode region remarkably decreases (about 50 cm^{-1}). Finally, high quality spectra in the overtone region show two broad absorption bands very similar in shape. By considering the position of the fundamental Raman and the dispersion of the infrared bands we are able to assign the two bands and to reproduce their profiles at all the experimental pressures. According to this fitting procedure it results a fundamental region composed by two separated density of states. The energy gap between the two DOS reaches a maximum around 20 GPa and decreases by further compression. To complete the vibrational information we also measured Raman spectra revealing an effect of the laser power on the peak position, especially for the L2 mode. This effect, which is also correlated to the excitation wavelength, is ascribed to the sample heating due to electronic absorption processes. All these vibrational data concerning the ϵ phase of solid oxygen can be consistently interpreted on the basis of a molecular crystal formed by O_4 molecules. The evolution of infrared frequencies and intensities suggests that the formation of the O_4 molecule is tuned by pressure and takes place between 10 and 20 GPa. A simple chain model provides accurate information on the interaction strength among neighboring O_4 molecules. This model reproduces the density of states of the high-frequency stretching modes of the O_4 molecule and represents an indirect proof of the correctness of our assignment, based on the results of an *ab initio* calculation. On the basis of the evolution with pressure of the characteristic force constants a polymeric association anticipating the insulator to metal transition can be excluded. The small structural changes which characterize the transition to metallic oxygen may suggest the fascinating hypothesis of a molecular metal composed by O_4 units.

ACKNOWLEDGMENTS

We are grateful to P.R. Salvi who provided us with the results of DFT calculations on the O_4 single molecule and to A. Painelli, G. Cardini, and V. Schettino for helpful discussions. This work has been supported by the European Union under Contract No. ERB FMGE CT 950017.

*Electronic address: gorelli@lens.unifi.it

†Electronic address: ulivi@ieq.fi.cnr.it

‡Electronic address: santoro@lens.unifi.it

§Electronic address: bini@chim.unifi.it

¹C. S. Yoo, H. Cynn, F. Gygi, G. Galli, V. Iota, M. Nicol, S. Carlson, D. Husermann, and C. Mailhot, Phys. Rev. Lett. **83**, 5527 (1999).

²M. Ceppatelli, M. Santoro, R. Bini, and V. Schettino, J. Chem.

- Phys. **113**, 5991 (2000).
- ³F. Moshary, N. H. Chen, and I. F. Silvera, Phys. Rev. B **48**, 12 613 (1993).
- ⁴H. Olijnyk and A. P. Jephcoat, Phys. Rev. Lett. **83**, 332 (1999).
- ⁵F. Gorelli, L. Ulivi, M. Santoro, and R. Bini, Phys. Rev. B **60**, 6179 (1999).
- ⁶M. Nicol, K. R. Hirsch, and W. B. Holzapfel, Chem. Phys. Lett. **68**, 49 (1979).
- ⁷H. d'Amour, W. B. Holzapfel, and M. Nicol, J. Phys. C **85**, 131 (1981).
- ⁸D. Schiferl, D. T. Cromer, and R. L. Mills, Acta Crystallogr., Sect. B: Struct. Crystallogr. Cryst. Chem. **37**, 1329 (1981).
- ⁹D. Schiferl, D. T. Cromer, L. A. Schwalbe, and R. L. Mills, Acta Crystallogr., Sect. B: Struct. Sci. **39**, 153 (1983).
- ¹⁰S. W. Johnson, M. Nicol, and D. Schiferl, J. Appl. Crystallogr. **26**, 320 (1993).
- ¹¹S. Desgreniers and K. E. Brister, in *High Pressure Science and Technology*, edited by W. A. Trzeciakowski (World Scientific, Singapore, 1996), p. 363.
- ¹²K. Shimizu, K. Sahara, M. Ikumo, M. I. Eremets, and K. Amaya, Nature (London) **393**, 767 (1998).
- ¹³Y. Akahama, H. Kawamura, D. Hausermann, M. Hanfland, and O. Shimomura, Phys. Rev. Lett. **74**, 4690 (1995).
- ¹⁴B. I. Swanson, S. F. Agnew, L. H. Jones, R. L. Mills, and D. Schiferl, J. Phys. Chem. **87**, 2463 (1983).
- ¹⁵M. Nicol and K. Syassen, Phys. Rev. B **28**, 1201 (1983).
- ¹⁶S. F. Agnew, B. I. Swanson, and L. H. Jones, J. Chem. Phys. **86**, 5239 (1987).
- ¹⁷G. N. Lewis, J. Am. Chem. Soc. **46**, 2027 (1924).
- ¹⁸L. Pauling, *The Nature of the Chemical Bond*, 3rd edition (Cornell University Press, Ithaca, 1960).
- ¹⁹C. A. Long and G. E. Ewing, Chem. Phys. Lett. **9**, 225 (1971).
- ²⁰J. G. Goodman and L. E. Brus, J. Chem. Phys. **67**, 4398 (1977).
- ²¹V. Aquilanti, D. Ascenzi, M. Bartolomei, D. Cappelletti, S. Cavalli, M. De Castro Vitores, and F. Pirani, Phys. Rev. Lett. **82**, 69 (1999).
- ²²P. E. S. Wormer and A. van der Avoird, Phys. Rev. Lett. **51**, 1167 (1983).
- ²³M. C. van Hemert, P. E. S. Wormer, and A. van der Avoird, J. Chem. Phys. **81**, 1229 (1984).
- ²⁴B. Bussery and P. E. S. Wormer, J. Chem. Phys. **99**, 1230 (1993).
- ²⁵V. Aquilanti, D. Ascenzi, M. Bartolomei, D. Cappelletti, S. Cavalli, M. De Castro Vitores, and F. Pirani, J. Am. Chem. Soc. **121**, 10 794 (1999).
- ²⁶F. Gorelli, M. Santoro, L. Ulivi, and R. Bini, Phys. Rev. Lett. **83**, 4093 (1999).
- ²⁷H. K. Mao, P. M. Bell, J. V. Shaner, and D. J. Steinberg, J. Appl. Phys. **49**, 3276 (1978).
- ²⁸R. Bini, R. Ballerini, G. Pratesi, and H. J. Jodl, Rev. Sci. Instrum. **68**, 3154 (1997).
- ²⁹R. Bini, M. Jordan, L. Ulivi, and H. J. Jodi, J. Chem. Phys. **108**, 6849 (1998).
- ³⁰Y. Akahama and H. Kawamura, Phys. Rev. B **61**, 8801 (2000).
- ³¹S. Califano, V. Schettino, and N. Neto, *Lattice Dynamics of Molecular Crystals* (Springer-Verlag, Berlin, 1981).
- ³²F. Gorelli, M. Santoro, L. Ulivi, and R. Bini, Phys. Rev. B **62**, R3604 (2000).
- ³³Y. Akahama and H. Kawamura, Phys. Rev. B **54**, 602 (1996).
- ³⁴F. Gorelli, M. Santoro, L. Ulivi, and R. Bini, Physica B **265**, 49 (1999).
- ³⁵All the values of the quantity χ reported in Table I of Ref. 26 should be multiplied by a factor of 10^4 which was erroneously missed in typing the manuscript.
- ³⁶H. Yamada and W. B. Person, J. Chem. Phys. **41**, 2478 (1964).
- ³⁷B. Olinger, R. L. Mills, and R. B. Roof, J. Chem. Phys. **81**, 5068 (1984).
- ³⁸S. Yoshida, K. Shimizu, T. Tokuda, T. Sawano, and T. Fujioka, Appl. Phys. Lett. **54**, 2400 (1989).
- ³⁹V. I. Dianov-Klokov, Opt. Spectrosc. **16**, 224 (1964).
- ⁴⁰D. J. Bernard, W. E. McDermott, and N. R. Pchelkin, Chem. Phys. Lett. **55**, 552 (1978).
- ⁴¹M. J. Frisch *et al.*, Gaussian, Inc., Pittsburgh, PA, 1995.
- ⁴²P. R. Salvi (private communication).
- ⁴³A. Painelli and A. Girlando, J. Chem. Phys. **84**, 5655 (1986).
- ⁴⁴R. J. Meier and R. B. Helmholtz, Phys. Rev. B **29**, 1387 (1984).
- ⁴⁵R. D. Eppers, K. Kobashi, and J. Belak, Phys. Rev. B **32**, 4097 (1985).
- ⁴⁶S. Serra, G. Chiarotti, S. Scandolo, and E. Tosatti, Phys. Rev. Lett. **80**, 5160 (1998).
- ⁴⁷K. Aoki, S. Usuba, M. Yoshida, Y. Kakudate, K. Tanaka, and S. Fujiwara, J. Chem. Phys. **89**, 529 (1988).
- ⁴⁸G. Turrell, *Infrared and Raman Spectra of Crystals* (Academic Press, London, 1972).